Journal Name

Dynamic Article Links ►

Cite this: DOI: 10.1039/c0xx00000x

www.rsc.org/xxxxxx

ARTICLE TYPE

Hydrogenation of tetralin over Pt catalysts supported on sulfated zirconia and amorphous silica alumina

Oliver Y. Gutiérrez,[a‡] Yanzhe Yu, [a‡] Robin Kolvenbach,[a] Gary L. Haller,[a] and Johannes A. Lercher [a]*

Received (in XXX, XXX) Xth XXXXXXXXX 20XX, Accepted Xth XXXXXXXXX 20XX

DOI: 10.1039/b000000x

Pt supported on sulfated zirconia (SZ) and amorphous silica alumina (ASA) was explored for the hydrogenation of tetralin. Pt/ASA had a higher concentration and strength of acid sites than the SZ-supported counterpart, for which the acid site concentration of the carrier decreases after catalyst synthesis due to sulfur elimination. The strong acidity of Pt/ASA caused higher deactivation due to coke deposition, while Pt/SZ was comparatively stable. Pt/ASA also exhibited higher porosity and Pt dispersion than Pt/SZ. The adsorption of CO, the XANES analysis and gravimetric sorption of benzene showed that the Pt particles on SZ were strongly electron deficient, a feature that has been speculated to be associated to the electron withdrawing effect of sulfate groups. For tetralin hydrogenation, Pt/SZ was more active than Pt/ASA above 423 K while the opposite was observed at 413 K. The apparent activation energies were 98 and 45 kJ/mol on Pt/SZ and Pt/ASA, respectively. Pt/ASA was more active than Pt/SZ in the presence of quinoline, while Pt/SZ retains the highest activity in the presence of dibenzothiophene (with or without quinoline). The lower apparent activation energy on Pt/ASA in the absence of quinoline or dibenzothiophene and its higher activity in the presence of quinoline were attributed to its strong Brønsted acidity, promoting the hydrogenation at the perimeter of Pt particles. The higher sulfur resistance of Pt/SZ was attributed to the electron deficiency of the supported Pt particles. In this respect, surface sulfate anions induce stronger electron deficiency in supported Pt than the acidity of the support.

Introduction

In order to achieve the high-quality diesel fuel required to meet present day environmental regulations, a two-stage process has been widely proposed.[1,2] In the first stage, metal sulfides, such as Co(Ni)-MoS_2, are used to minimize the content of heteroatoms, whereas in the second stage deep hydrogenation of aromatics is conducted on supported noble metals. These noble metal-based catalysts exhibit high hydrogenation activity at relatively mild reaction conditions, but the rates observed with these catalysts is dramatically reduced by competitive adsorption of molecules containing heteroatoms and the associated partial sulfidation of the metal particles.[3] These negative effects can be reduced by using acidic supports, which is attributed to electronic transfer from noble metal particles towards the support.[3-7] Additionally, Brønsted acid sites at the perimeter of the metal particles may facilitate the hydrogenation of aromatics.[6-9]

Sulfated zirconia (SZ) is an acidic solid suitable for catalyzing numerous reactions at remarkably low temperatures.[10] Few papers have addressed the hydrogenation activity of Pt supported on SZ,[11,12] probably due to the acid-catalyzed reactions occurring on the latter, which makes it difficult to exclusively study the hydrogenation properties of supported Pt. It is established that SZ-supported Pt particles are electron deficient due to their interaction with sulfur species of the support.[13-16,] Thus, we expected that supported Pt exhibits outstanding hydrogenation activity even in the presence of sulfur and nitrogen containing molecules. In the present work, we study the hydrogenation activity and poison resistance of Pt particles supported on sulfated zirconia using model compounds. The properties and performance of Pt/SZ are compared to Pt supported on amorphous silica alumina (ASA), whose hydrogenation performance has been studied in more detail.[7-9]

Experimental

Catalyst preparation

Sulfated zirconia (MEL Cat, XZO 1249) and ASA (Sasol Germany, SIRAL 30, SiO_2/Al_2O_3 weight ratio of 70/30) were used as supports. SZ and ASA were thermally treated in air at 873 K for 3 h, and 823 K for 4 h, respectively. After those treatments, both materials were impregnated with aqueous solutions of $Pt(NH_3)_4(NO_3)_2$ (Aldrich, 99.995%), dried and treated consecutively in flowing air at 673 K for 2 h and in hydrogen at 623 K for 4 h. The nominal Pt loading in both catalysts was 0.8 wt.%. The Pt catalysts supported on sulfated zirconia and ASA are denoted in the following as Pt/SZ and Pt/ASA, respectively.

Table 1. Physicochemical properties of supports and catalysts.

Support or catalyst	BET Surface area ($m^2 \cdot g^{-1}$)	Pt content (wt.%)	Pt particle size[1] (nm)	Pt particle size[2] (nm)	Acid site concentration ($\mu mol \cdot g^{-1}$)			
					BAS		LAS	
					Total	Strong	Total	Strong
SZ	165	-	-	-	139	86	256	135
Pt/SZ	165	0.81	2.3	1.7	26	8	343	153
ASA	481	-	-	-	56	29	526	246
Pt/ASA	423	0.793	1.1	1.3	41	25	387	234

[1] Mean metal particle sizes calculated as C/D, where C is 1.13 for Pt and D is the dispersion calculated from H_2 chemisorption.[21]
[2] Metal particle sizes calculated from TEM measurements.

Catalyst characterization

The concentration of Pt in the catalysts was determined by atomic absorption spectroscopy (AAS) using a UNICAM 939 spectrometer. Carbon and sulfur contents of fresh and spent catalysts were determined using a Vario EL analyzer (ELEMENTAR). The texture of supports and catalysts were determined from N_2 adsorption measurements carried out at 77 K using a PMI automated BET sorptometer. Prior to the measurements, all materials were outgassed at 523 K for 20 h. Specific surface areas and porosities were calculated applying BET and BJH theories, respectively. The dispersion of Pt was measured by H_2 chemisorption at 298 K after activation in vacuum at 588 K for 1 h. Two adsorption isotherms were measured from 1 to 40 kPa, that is, before and after outgassing at 298 for 1 h. The metal dispersion was estimated from the concentration of chemisorbed hydrogen, calculated by subtracting the second isotherm from the first one. The average particle sizes of Pt particles in the catalysts were measured by TEM. Samples were ground, suspended in ethanol and ultrasonically dispersed and the dispersion drops were applied on a copper-carbon grid. Measurements were carried out on a transmission electron microscope device JEOL JEM-2011 with an accelerating voltage of 120 keV.

Infrared spectra of adsorbed pyridine and CO were measured to characterize the acidity of the materials and properties of the supported metal, respectively. The adsorption of pyridine was monitored with a Perkin Elmer 2000 spectrometer operating at a resolution of 4 cm^{-1}. Prior to the pyridine sorption experiments, the catalyst samples were activated at 10^{-6} mbar and 723 K for 1 h. The activated samples were exposed to pyridine ($p_{(Py)} = 10^{-1}$ mbar) at 423 K for 0.5 h and after evacuation at 423 K for 1 h the IR spectra were recorded. These spectra corresponded to pyridine adsorbed on all acid sites. Afterwards, the samples were heated at 723 K in vacuum for 1 h and another series of spectra was collected corresponding to pyridine adsorbed on strong acid sites. The concentration of weak acid sites was determined by subtracting both series of spectra. The concentrations of Lewis (LAS) and Brønsted (BAS) acid sites were quantified using the molar extinction coefficients of 0.965 and 0.726 cm μmol^{-1} respectively.[17] The adsorption of CO was measured using a Bruker VERTEX 70 with a resolution of 2 cm^{-1}. The catalysts were activated in H_2 for 1 h followed by evacuation ($p = 10^{-6}$ mbar) for 1 h at 623 K. Then, the catalysts were cooled to 313 K, outgassed for 15 minutes and finally CO was adsorbed at a pressure of 0.5 mbar.

Temperature programmed reduction (TPR) was applied to study changes in un-reduced Pt/SZ during the synthesis steps. After impregnation of the Pt precursor on SZ and thermal treatment in air, 0.2 g of the material was heated to 1073 K in a H_2 flow ($10ml \cdot min^{-1}$) with a heating rate of 3 $K \cdot min^{-1}$. A mass spectrometer (Balzers QME 200) was used for monitoring the evolved gases.

X-ray absorption spectra were collected at the beamlines X1 at HASYLAB, DESY, Hamburg, Germany. The storage ring was operated at 4.5 GeV at an average current of 100 mA. The Si (311) double crystal monochromator was detuned to 60% of the maximum intensity to minimize the intensity of higher harmonics in the X-ray beam. Self-supporting wafers of the catalysts were first reduced with H_2 in situ at 623 K for 1 h and then flushed with He at 623 K for 0.5 h to remove adsorbed H_2. The X-ray absorption spectra were collected at the Pt L_{III} edge (11564 eV) at 77 K. The position of the edge was calibrated using the spectra of a simultaneously measured Pt foil. The scattering contributions in the pre- and post-edge of the background were removed from the X-ray absorption using a third-order polynomial function and afterwards all spectra were normalized to the average post-edge height of one in the region of 11564 eV above the edge. The XANDA programs were used for analyzing the data.[18]

In order to explore the adsorption of aromatics on the catalysts, gravimetric sorption isotherms of benzene on Pt/ASA and Pt/SZ were measured in a Seteram TG-DSC 111 thermoanalyzer connected to a high vacuum system. Samples of the reduced materials (approximately 20 mg) were placed in a quartz sample holder and activated at 523 K for 1h under vacuum ($p<10^{-4}$ mbar) with an incremental heating rate of 10 $K \cdot min^{-1}$. The equilibration with the sorbate was performed in small pressure steps from $3 \cdot 10^{-2}$ to 1.2 mbar, whereas the mass increase and the thermal flux were measured. The overall heat of adsorption was obtained by integration of the observed heat flux signal. In order to obtain the maximum uptake, and enthalpy and entropy of adsorption on the metal site phase and the support, the data was analyzed according to the dual site Langmuir formalism shown in Eq. i, where n(p) is the adsorbed amount, K_i is the adsorption equilibrium constant, p is the pressure of benzene and $n_{max,i}$ is the maximum coverage on the metal phase or the support (denoted by i). In order to reduce the number of parameters, the enthalpy (ΔH) and entropy (ΔS) of adsorption were used as parameters for the fitting procedure according to Eq. ii. Nonlinear parameter fitting was carried out using a CMA evolutional strategy implemented in MATLAB.[19]

$$n(p) = \sum \frac{K_i * p * n_{max,i}}{1 + K_i * p} \qquad \text{(i)}$$

$$K_i = \exp\left(-\frac{\Delta H_{ads,i}}{RT}\right) * \exp\left(\frac{\Delta S_{ads,i}}{R}\right) \qquad \text{(ii)}$$

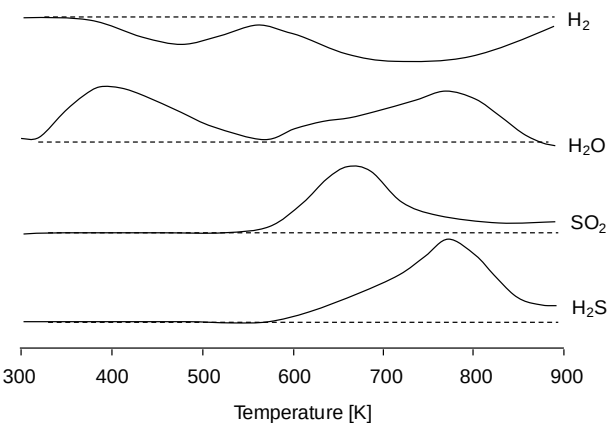

Fig. 1 Temperature programmed reduction profiles of H_2O, SO_2 and H_2S of un-reduced Pt/SZ.

Activity test

Hydrogenation of tetralin in the absence and presence of quinoline and dibenzothiophene (DBT) was used as a model reaction to investigate the catalytic activities of Pt/SZ and Pt/ASA. The reactions were carried out in a set of 4 parallel trickle-bed reactors in continuous down-flow mode.[20] The activity tests were carried out at 413-503 K and 50 bar H_2 with a weight hourly space velocity (WHSV) of 1500 h^{-1} for poison-free feed (i.e., without quinoline or dibenzothiophene), of 300 h^{-1} for feed containing quinoline, 60 h^{-1} for DBT-containing feed, and 21 h^{-1} for feed containing quinoline and DBT (WHSV is defined as the weight of feed per hour per unit weight of catalyst). The change in WHSV was achieved by varying the amount of catalyst and the flow rate keeping a constant molar ratio of H_2 to tetralin of 75. The poison-free feed consisted of 5 wt.% tetralin, and 5 wt.% hexadecane as GC standard in tetradecane. In catalytic experiments in the presence of DBT or quinoline in separate tests, 0.058 wt.% DBT and 0.37 wt.% quinoline was used, whereas in the experiments with both compounds 0.019 and 0.058 wt.% quinoline and DBT, respectively, were used. Continuous deactivation was observed in all reactions in the first 20 h time on stream (TOS) of the reaction. Thus, all catalytic activities here reported were collected at steady state after 24 h of time TOS.

Results and discussion

Physicochemical properties of supports and catalysts

The physicochemical properties of supports and catalysts are summarized in Table 1. Compared to the respective supports, the specific surface area of Pt/SZ did not change, that of Pt/ASA slightly decreased. The H/Pt ratios were 0.50 and 1.07 for Pt/SZ and Pt/ASA, respectively. The corresponding average Pt particle sizes have been estimated to be 2.3 nm for Pt/SZ and 1.1 nm for Pt/ASA.[21] The average particle size derived from TEM measurements was 1.3 nm for Pt/ASA, i.e., larger than that determined from H_2-chemisorption. Most probably, the smaller metal particles escaped detection during analysis of the TEM images causing the overestimation of the average particle size. In contrast, for Pt/SZ, the Pt particle size derived from TEM was 1.7 nm, i.e., smaller than that determined from chemisorbed H_2. This is attributed to partial coverage of Pt particles by sulfur released from the carrier and reduced during the synthesis steps (vide infra), which blocked to some extent the adsorption of H_2. The dispersion of Pt/ASA was higher than that of Pt/SZ likely due to the higher specific surface area and concentration of Lewis acid sites on the former support, which are likely anchoring sites for Pt particles.[22]

The Brønsted and Lewis acid site concentrations on ASA decreased during the preparation of the Pt catalyst. For Pt/SZ, the concentration of Brønsted acid sites decreased drastically, whereas the concentration of Lewis acid sites increased after Pt loading. Both observations are attributed to dehydration and decomposition of sulfate groups during the thermal treatments. Reactions (1) and (2) have been proposed for the creation of Lewis acid sites.[23,24] Accordingly, the sulfur content of the as-synthesized Pt/SZ was lower than that of the pure support (1.50 and 2.14 wt. %, respectively). It is important to mention that the concentration of Brønsted sites is not a simple function of the sulfur concentration as it seems that isolated sulfate species do not produce Brønsted acidity.[25,26]

$$HSO_4^- + Zr\text{-}OH \rightarrow SO_4^{2-} + H_2O \quad (1)$$

$$2Zr^{4+} + SO_4^{2-} \rightarrow 2Zr^{3+} + SO_2 + O_2 \quad (2)$$

The evolution profiles of H_2O, SO_2 and H_2S recorded during TPR of not-reduced Pt/SZ are shown in Figure 1. The units in the Figure are arbitrary, however, the release-uptake profiles allow a qualitative description of the phenomena involved in TPR. Hydrogen exhibits two consumption signals in the ranges of 370-570 K, and 570-900 K. The water evolution signal below 600 K is attributed to the desorption of physisorbed water (maximum at 380 K) and the reduction of Pt oxide species (in the range of low temperature H_2-consumtpion[27,28]) according to reaction (3). Water desorption above 600 K is coupled with the release of SO_2 and H_2S, with maxima at 670 and 770 K, respectively. The release of these two compounds was attributed to elimination of surface sulfate groups as SO_2 at low temperature and H_2S at high temperature due to Pt-catalyzed SO_2 reduction[29] as shown in Reaction (4). Alternatively, the two different decomposition mechanisms presented in Reactions (5) and (6) have also been proposed.[30] These results indicate that surface sulfate groups are eliminated from Pt/SZ during the synthesis and, therefore, the Brønsted acidity decreases because the concentration of Brønsted acid sites depends on the concentration of surface sulfates.[31] Conversely, the concentration of Lewis acid sites increased with the thermal treatment due to the conversion of Brønsted into Lewis acid sites on the removal of chemisorbed water and SO_4^{2-}.[10]

$$PtO_x + xH_2 \rightarrow Pt + xH_2O \quad (3)$$

$$SO_2 + 3H_2 \rightarrow H_2S + 2H_2O \quad (4)$$

$$Zr\text{-}SO_4\text{-}Zr + 4H_2 \rightarrow Zr\text{-}O\text{-}Zr + H_2S + 3H_2O \quad (5)$$

$$Zr\text{-}SO_4\text{-}Zr + H_2 \rightarrow Zr\text{-}O\text{-}Zr + SO_2 + H_2O \quad (6)$$

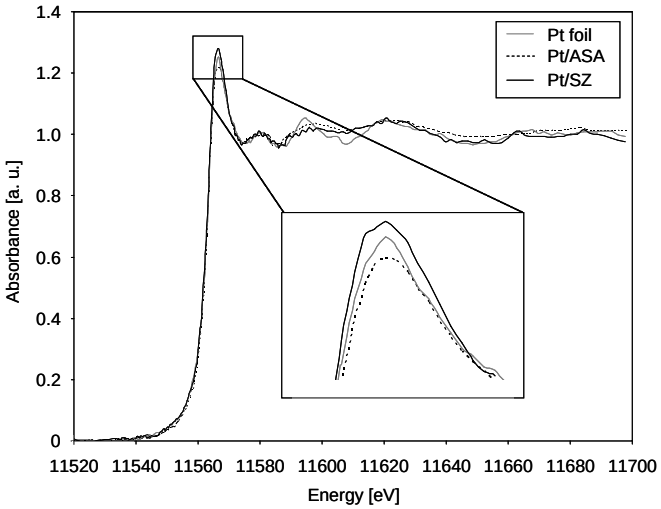

Fig. 2 Normalized XANES at the Pt LIII edge in He at 623 K of Pt foil and Pt/ASA, Pt/SZ catalysts after in situ reduction in H_2 at 623 K.

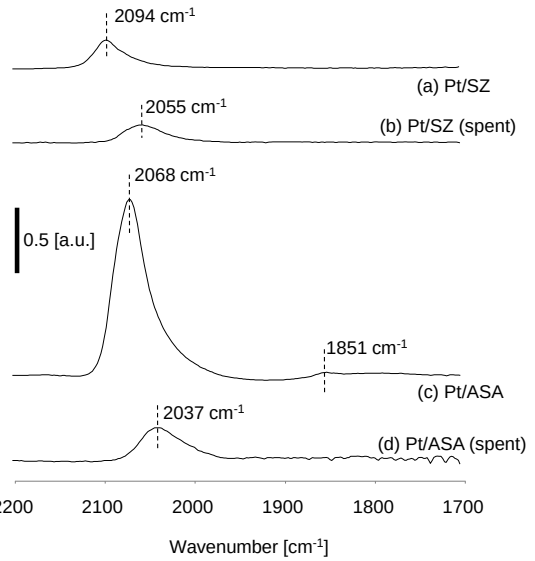

Fig. 3 IR spectra of CO adsorbed on (a) Pt/SZ, (b) spent Pt/SZ, (c) Pt/ASA and (d) spent Pt/ASA catalysts at T = 40 ºC, p(CO) = 5•10-1 mbar and evacuation for 15 min. Spent catalysts (b) and (d) were Pt/SZ and Pt/ASA after TOS of 24 h in tetralin hydrogenation reaction (p = 50 bar, T = 453 K, in poison-free feed).

Characterization of the Pt particles

The electronic states of Pt particles in the catalysts were compared to that in bulk Pt by X-ray absorption spectroscopy (Figure 2). The integrated intensities of the XANES at the Pt L_{III} edge were obtained by calculating the area enclosed between the XANES and a sigmoidal function fitting the edge.[32] The intensities were 1.52, 0.99, and 1.27 a.u. for Pt/SZ, Pt/ASA and Pt foil, respectively. It is known that the XANES intensity is proportional to the hole density at the $5d_{5/2}$ and $5d_{3/2}$ states of Pt. Therefore, the differences in the white line intensities in Fig. 2 and the integrated XANES area indicate a lower electron density of Pt on sulfated zirconia compared to bulk and ASA supported Pt.

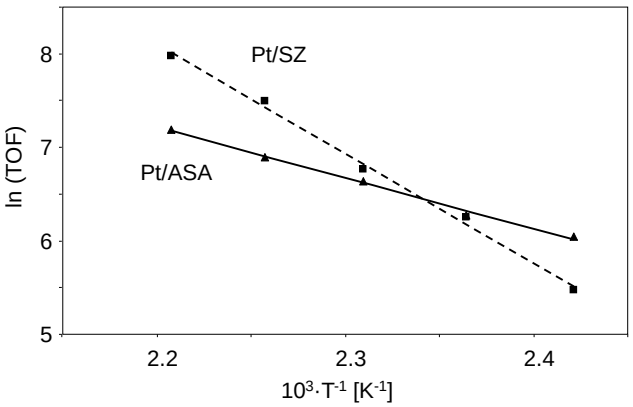

Fig. 4 Arrhenius plots for the hydrogenation of tetralin over Pt/SZ and Pt/ASA at 50 bar H_2 and 413-453K.

The Pt particles of Pt/SZ and Pt/ASA were further characterized by IR spectra of adsorbed CO. In Fig. 3, spectra (a) and (c) correspond to CO adsorbed on as-reduced Pt/SZ and Pt/ASA. Bands observed at 2094 and 2068 cm^{-1} for Pt/SZ and Pt/ASA, respectively, are attributed to CO linearly adsorbed on Pt.[33] Additionally, a low-intensity band at 1851 cm^{-1}, observed for Pt/ASA, was assigned to bridging CO adsorbed on Pt.[34] The higher wavenumber of CO adsorbed on Pt/SZ than on Pt/ASA indicated weaker CO adsorption likely due to relatively low electron density of Pt in the former catalyst.[34] Additionally, the normalized area of linearly adsorbed CO on Pt/ASA was significantly higher than that of Pt/SZ, which is attributed to the higher dispersion of Pt in Pt/ASA and to the partial coverage of the metal particles on SZ by sulfur removed from the carrier during the synthesis.

Hydrogenation of tetralin on Pt/SZ and Pt/ASA in the absence of quinoline and DBT

The hydrogenation of tetralin was carried out from 413 to 503 K. In this temperature range only hydrogenated products were observed. Figure 4 shows the temperature dependence of turnover frequency (TOF) of the hydrogenation of tetralin on Pt/SZ and Pt/ASA. The former is more active above 423 K than the latter. At 423 K both catalysts have the same activity and, at the temperatures at which the reaction was measured, only at 413 K Pt/ASA is more active than Pt/SZ. The apparent activation energies ($E_{a(exp)}$) were 98 and 45 kJ/mol on Pt/SZ and Pt/ASA, respectively.

$E_{a(exp)}$ includes the contribution of the intrinsic activation energy (E_a) and the adsorption enthalpies (ΔH_i) of the reactants, according to the Temkin equation (3), where n_i are the reaction orders (*i* is T and H for tetralin and hydrogen, respectively). The intrinsic activation barrier and rate limiting step are likely the same on both catalysts.[33] The reaction is first order in tetralin,[7] whereas for hydrogen, the reaction order is positive, around one.[36,37] The adsorption enthalpies of tetralin and hydrogen depend on the electronic state of the Pt particles. However, it is important to note that neither the influence of ΔH_T nor that of ΔH_H on $E_{a(exp)}$ can be neglected, because both have similar magnitudes (although the former is larger than the latter).[38]

$$E_{a(exp)} = E_a + n_T\Delta H_T + n_H\Delta H_H \quad (3)$$

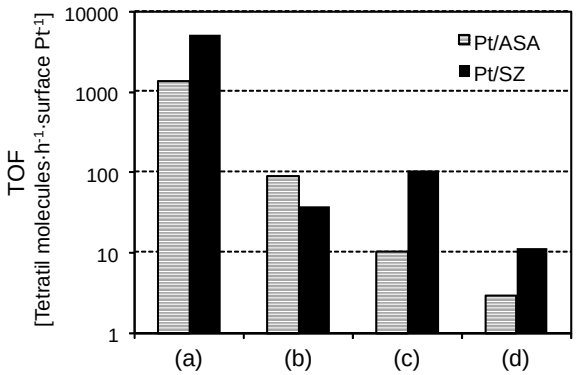

Fig. 5 Turnover frequency (TOF) observed in the hydrogenation of tetralin in the absence of heterocompounds (a), in the presence of quinoline (b), dibenzothiophene (c), and quinoline and dibenzothiophene (d). All the activities were measured at 503 K and 50 bar H_2 after 24 h TOS.

Table 2. Adsorption enthalpies and entropies derived from the gravimetric sorption isotherms of benzene on Pt/ASA and Pt/SZ. The subscripts "sup" and "Pt" denote the parameters corresponding to adsorption on the support and on Pt respectively.

Catalyst	$\Delta H_{ads,\ sup.}$ ($kJ \cdot mol^{-1}$)	$\Delta H_{ads,Pt.}$ ($kJ \cdot mol^{-1}$)	$\Delta S_{ads,\ sup.}$ ($J \cdot mol^{-1} \cdot K^{-1}$)	$\Delta S_{ads,\ Pt.}$ ($kJ \cdot mol^{-1} \cdot K^{-1}$)
Pt/SZ	64	73	121	116
Pt/ASA	47	52	86	65

Table 3. Elemental analysis of fresh and spent Pt/SZ and Pt/ASA.

Support or catalyst	C content of fresh sample (wt.%)	C content of spent sample [1] (wt.%)	S content of fresh sample (wt.%)	S content of spent sample [1] (wt.%)
SZ	<0.1	-	2.14	-
Pt/SZ	<0.1	2.88	1.50	1.40
ASA	0.11	-	-	-
Pt/ASA	0.12	10.50	-	-

[1]Spent catalyst after tetralin hydrogenation (453 K, 50 bar H_2, 48h TOS)

The enthalpies of adsorption for tetralin, dibenzothiophene or quinoline were not accessed in this work. However, the enthalpies of adsorption of benzene on the catalysts provided insight into the interaction of aromatic compounds on metal with varying electronic deficiencies. Table 2 shows the values of adsorption enthalpies and entropies derived from the gravimetric sorption isotherms of benzene on the catalysts. The enthalpy of adsorption of benzene on Pt/SZ was higher than on Pt/ASA (73 and 52 $kJ \cdot mol^{-1}$, respectively). This is explained by a stronger interaction of the aromatic ring with the Pt on SZ that is more electron deficient that the Pt on ASA. The entropy of of adsorption on Pt was also higher on Pt/SZ than on Pt/ASA (116 and 62 $kJ \cdot mol^{-1} \cdot K^{-1}$, respectively) likely due to the greater entropy losses associated with stronger sorbate-adsorbent interactions. This phenomenon has been referred as the compensation effect.[39,40]

Similarly to the adsorption of benzene on the Pt particles, the enthalpy of adsorption of tetralin has to be higher on Pt/SZ than on Pt/ASA because stronger adsorption of on more electron deficient Pt particles is expected for all aromatic molecules. Indeed, the covalent character of the interaction between aromatics and d-metals is much larger on a metal with a partially occupied d-band than on one with an fully occupied d-band.[41] In a recent report, tetralin and benzothiophene were adsorbed on a series of Pt catalysts supported on MCM-41 modified with different concentrations of aluminium.[42] The uptake of both compounds and its interaction strength with the catalyst increased with the addition of Al and the concomitant increase of support acidity. This observation is explained by increasing cationic character of the supported Pt, which is consistent with our view.

However, as the hydrogenation at the perimeter of Pt particles has an important contribution to the overall process,[20,43] strong adsorption on Brønsted sites on ASA (due to higher concentration and strength than on SZ) would compensate to some extent the weaker adsorption on the metal surface. Unfortunately, the thermodynamic parameters reported in Table 2 concerning adsorption on the support do not allow us to conclude at this respect because at the temperatures used in the adsorption experiments, the adsorption isotherms include contributions of benzene adsorbed in the whole surface of the supports and not only on acid sites.

The adsorption of H_2 on Pt, on the other hand, weakens as the electron deficiency of the metal increases,[44] and therefore, ΔH_H has to be less negative with Pt/SZ than with Pt/ASA. Thus, it is reasonable to conclude that the adsorption of tetralin on Brønsted sites and adsorption of hydrogen on electron-deficient Pt lead to lower $E_{a(exp)}$ on Pt/ASA than on Pt/SZ.

The extent of coke deposition on the catalysts was explored by comparing the elemental composition and IR spectra of adsorbed CO on the catalysts before and after reaction. Table 3 shows that the carbon content increases in both catalysts, from traces to 2.88 and 10.5 wt.% in Pt/SZ and Pt/ASA, respectively. This confirms that deactivation, observed mainly within the first 24 h TOS, is due to coke deposition. The concentration of sulfur during the reaction is reduced from 1.5 to 1.4 wt. %.

The band of adsorbed CO in the spectra of the spent catalysts (Figure 3) shifted to lower wavenumbers compared to the fresh catalysts, i.e., from 2068 to 2037 cm^{-1} for Pt/ASA and from 2094 to 2055 cm^{-1} for Pt/SZ. This red shift is attributed to the presence of coke, which donates negative charge to Pt particles increasing the back donation to adsorbed CO molecules. Coke forms on the metal as inferred from the strong decrease of the CO band intensities. Estimating the decrease of the band, 76% of the metal surface remained available for CO adsorption for Pt/SZ, while on Pt/ASA only 21% of the metal surface was still exposed after the reaction. The dramatic decrease of metal area in Pt/ASA is in line with the significant carbon deposition most likely due to the high acidity of the material.

The hydrogenation activities of both catalysts at 503 K with a clean feed, in the presence of quinoline, DBT and both compounds are compared in Fig. 5. It is important to mention that taking into account the decrease of exposed metal surface in the spent catalysts (that is, 24% and 79% in Pt/SZ and Pt/ASA, respectively) the TOF values increase, especially those of Pt/ASA (not shown). However, the trends are preserved and thus the discussion here presented is valid for the catalysts during reaction conditions.

In the absence of heterocompounds, Pt/SZ is more active than Pt/ASA. The most abundant product was cis-decalin, whereas the

cis- to trans-decalin ratio was nearly the same on both catalysts at the same conversion levels.

The hydrogenation activity of the two catalysts decreased by orders of magnitude with the addition of quinoline or DBT, especially in the presence of both. Pt/ASA is more active than Pt/SZ in the presence of quinoline, whereas Pt/SZ is the most active in the presence of DBT (in the presence or absence of quinoline). In all cases, the cis- to trans-decalin ratios decreased, compared to that observed in the absence of heterocompounds. This indicated that their presence reduced the strength between tetralin and Pt, either by competitive adsorption or by changing the electronic state. Quinoline was completely converted when present in the feed. The conversion of DBT was 67 and 51% over Pt/SZ and Pt/ASA, respectively, in the absence of quinoline and 20% on both catalysts in the presence of quinoline.

Apart from competitive and strong adsorption, S- and N-containing compounds impose inhibiting effects on specific sites. That is, desulfurization poisons the metal surface via the formation of a sulfide layer, whereas N-containing compounds neutralize the Brønsted sites at the perimeter. Pt/ASA has higher concentration of Brønsted acid sites and, therefore, may keep higher hydrogenation activity in the presence of quinoline than Pt/SZ (where neutralization of acid sites would require lower concentration of N-containing compounds). In the presence of DBT, however, Pt/SZ maintains the highest hydrogenation ability, likely due to relatively low sulfur poisoning originated from weak Pt-S interaction. In turn, this sulfur resistance must be attributed to the higher electron deficiency of Pt on SZ than on ASA (as concluded from XANES and IR of adsorbed CO).

The electronegativity and acidity of ASA are higher than that of sulfated zirconia, both properties being correlated with the electron deficiency of supported metal particles.[5,8,9] Therefore, the much higher electron deficiency on SZ than on ASA is attributed to the interaction of the metal particles with sulfur in the support.[13,45,46] It is interesting to note that the electronic deficiency of Pt on sulfated zirconia, i.e., higher than in the reference Pt foil is similar to that observed when Pt is alloyed with Pd.[43,47] Therefore, the electron-withdrawing effect of sulfated zirconia is speculated to be similar in magnitude to that imposed by alloying.

The nature of the interaction of the metal particles with the SZ is controversial. Several groups have proposed that Pt is at least partially sulfided on SZ.[48,49] There are also indications that the cationic character of Pt on SZ is due to Pt-O interactions and therefore Pt-PtO_x core-shell models have been proposed.[45,46] On the other hand, the presence of sulfate groups seems to aid the reduction of oxide Pt species.[50] Therefore, we are inclined to believe that sulfur partially blocks the metal surface[29] and that some remaining Pt-O-S bonds, which could also explain the finding of Pt-O contributions in literature, ease the electronic withdrawing from Pt towards the surface sulfate groups. Although more work is needed to differentiate the contributions of these two mechanisms, the occurrence of both lead to strong electron deficiency of Pt on SZ.

Conclusions

Pt catalysts (0.8 wt.% of Pt), supported on sulfated zirconia (SZ) and amorphous silica alumina (ASA), were synthesized, characterized and tested in hydrogenation of tetralin. The higher textural and acid properties of ASA led to higher Pt dispersion of Pt/ASA than of Pt/SZ. Compared to the respective supports, the acidity remained constant for Pt/ASA. For Pt/SZ, however, the Brønsted acidity decreased, and Lewis acidity increased due to elimination of sulfur during the synthesis. The net outcome was that the concentration and strength of acid sites was higher on Pt/ASA than on Pt/SZ, which led to stronger deactivation of the former due to coke formation (more than twice in Pt/ASA than in Pt/SZ according to elemental analysis and CO-adsorption).

The Pt particles on SZ were more electron deficient than that on ASA or Pt foil according to adsorption of CO followed by IR spectroscopy (on SZ, the bond vibrations of adsorbed CO appear at the highest wavelengths), XANES analysis (the whiteline of the Pt edge is the most intense for Pt/SZ) and gravimetric sorption of benzene. This electron deficiency in Pt/SZ was attributed to the electron-withdrawing effect of sulfate groups on the support.

In the tetralin hydrogenation in absence of poisons Pt/SZ was more active than Pt/ASA above 423 K, whereas the latter was more active than the former at 413 K. At 503 K, in the presence of quinoline, Pt/ASA was more active than Pt/SZ, due to its higher concentration of Brønsted acid sites, which increased its resistance to neutralization by N-containing compounds. In the presence of dibenzothiophene Pt/SZ retained higher activity than Pt/ASA due to the higher electron deficiency of the former which provided better sulfur resistance. This study shows that inducing electron deficiency in supported Pt particles is crucial to obtain active hydrogenation catalysts, especially in the presence of sulfur-containing compounds. The presence of surface sulfate anions may induce stronger electron deficiency on supported Pt than the acidity of the support avoiding the drawback of deactivation due to coke deposition.

Acknowledgements

The authors thank MEL Cat and Sasol Germany for providing the sulfated zirconia and amorphous silica alumina supports. Parts of this research were carried out at the light source facility DORIS III at DESY, a member of the Helmholtz Association (HGF). The authors are grateful to the HASYLAB staff for their kind assistance during the experiments at the beamline X1.

Notes and references

[a] *Lehrstuhl für Technische Chemie 2,Technische Universität München, Lichtenbergstraße 4, D-85747 Garching, Germany. Fax:+49/89/28913544. E-mail: johannes.lercher@ch.tum.de*

[‡] *These authors contributed equally to this work.*

1 A. Stanislaus, B. H. Cooper, *Catal. Rev. Sci. Eng.*, 1994, **36**, 75-123.
2 B. H. Cooper, B. B. L. Donnis, *Appl. Catal. A.*, 1996, **137**, 203-223.
3 J. Barbier, E. Lamy-Pitara, P. Marecot, J.P. Boitiaux, J. Cosyns, F. Verna, *Adv. Catal.*, 1990, **37**, 279-318.
4 H. Yasuda, T. Sato, Y. Yoshimura, *Catal. Today*, 1999, **50**, 63-71.
5 D. Poondi, M. A. Vannice, *J. Catal.*, 1996, **161**, 742-751.
6 J. Wang, L. M. Huang, Q. Li, *Appl. Catal. A*, 1998, **175**, 191-199.
7 M. F. Williams, B. Fonfé, A. Jentys, C. Breitkopf, J. A. R. van Veen, J. A. Lercher, *J. Phys. Chem. C*, 2010, **114**, 14532-14541.
8 M. F. Williams, B. Fonfé, C. Sievers, A. Abraham, J. A. van Bokhoven, A. Jentys, J. A. R. van Veen, J.A. Lercher, *J. Catal.*, 2007, **251**, 485-496.

9 M.F. Williams, B. Fonfé, C. Woltz, A. Jentys, J. A. R. van Veen, J. A. Lercher, *J. Catal.*, 2007, **251**, 497-506.
10 G. D. Yadav, J. J. Nair, *Micro. Meso. Mat.*, 1999, **33**, 1-48.
11 J. van Gestel, V. T. Nghiem, D. Guillaume, J. P. Gilson, J. C. Duchet, *J. Catal.*, 2002, **212**, 173-181.
12 K. Shimizu, T. Sunagawa, C. R. Vera, K. Ukegawa, *Appl. Catal. A*, 2001, **206**, 79-86.
13 T. Tanaka, T. Shishido, H. Hattori, K. Ebitani, S. Yoshida, *Physica B*, 1995, **208**, 649-650.
14 K. Ebitani, T. Tanaka, H. Hattori, Appl. Catal. A 102 (1993) 79-92.
15 Z. Paál, M. Muhler, R. Schlögl, J. Catal. 143 (1993) 318-321.
16 T. Shishido, T. Tanaka, H. Hattori, J. Catal. 172 (1997) 24-33.
17 S. Maier, A. Jentys, J. A. Lercher, J. Phys. Chem. C, 115 (2011) 8005.
18 K. V. Klementiev, *VIPER and XANDA for Windows, freeware*
19 N. Hansen, in *Towards a New Evolutionary Computation. Advances on Estimation of Distribution Algorithms* (Eds.: J. A. Lozano, P. Larranaga, I. Inza, E. Bengoetxea), Springer, New York, **2006**, p. 75.
20 Y. Yu, B. Fonfé, A. Jentys, G. L. Haller, J. A. R van Veen, O. Y. Gutiérrez, J. A. Lercher, *J. Catal.*, 2012, **292**, 13-25.
21 M. Choi, Z. Wu, E. Iglesia, *J. Am. Chem. Soc.*, 2010, **132**, 9129-9137.
22 J. H. Kwak, J. Z. Hu, D. H. Mei, C. W. Yi, D. H. Kim, C. H. F. Peden, L. F. Allard, J. Szanyi, *Science*, 2009, **325**, 1670-1673.
23 A. Clearfield, G.P.D. Serrete, A.H. Khazi-Syed, Catal. Today 20 (1994) 295.
24 F.R. Chen, G. Coudurier, J.F. Joly, J.C. Vedrine, J. Catal. 143 (1993) 616.
25 C. Monterra, G. Cerrato, C. Emanuel, V. Bolis, J. Catal. 142 (1993) 349
26 X.B. Li, K. Nagaoka, R. Olindo, J.A. Lercher, J. Catal. 238 (2006) 39
27 J. R. González-Velasco, M. A. Gutiérrez-Ortiz, J. A. González-Marcos, P. Pranda, P. Steltenpohl, *J. Catal*., 1999, **187**, 24-29.
28 D. L. Hoang, S. A. -F. Farrage, J. Radnik, M. -M. Pohl, M. Schneider, H. Lieske, A. Martin, *Appl. Catal., A* 2007, **333**, 67-77.
29 B. Q. Xu, W. M. H Sachtler, *J. Catal*., 1997, **167**, 224-233.
30 A. Dicko, X. Song, A. Adnot, A. Sayari, J. Catal. 150 (1994) 254
31 K. Föttinger, K. Zorn, H. Vinek, *Appl. Catal., A* 2005, **284**, 69-75.
32 A. Jentys, M. Englisch, G. L. Haller, J. A. Lercher, *Catal. Lett.*, 1993, **21**, 303-308.
33 P. Chou, A. Vannice, *J. Catal.*, 1987, **107**, 140-153.
34 C. M. Grill, M. L. McLaughlin, J. M. Stevenson, R. D. Gonzalez, *J. Catal.*, 1981, **69**, 454-464.
35 B. Coq, C. Walter, R. Brown, G. McDougnall, F. Figuéras, Catal. Lett. 39 (1996) 197-203.
36 T. C. Huang, B. C. Kang, *Ind. Eng. Chem. Res.*, 1995, **34**, 1140-1148.
37 T. Fujikawa, K. Idei, K. Ohki, H. Mizuguchi, K. Usui, *Appl. Catal. A*, 2001, **205**, 71–77.
38 R. C. Santana, S. Jongpatiwut, W. E. Alvarez, D. E. Resasco, *Ind. Eng. Chem. Res.*, 2005, **44**, 7928-7934.
39 B. A. De Moor, M. F. Reyniers, O. C. Gobin, J. A. Lercher, G. B. Marin, *J. Phys. Chem. C*, 2011, **115** 1204-1219.
40 F. Eder, M. Stockenhuber, J. A. Lercher, *J. Phys. Chem. B*, 1997, **101**, 5414-5419.
41 W. Liu, J. Carrasco, B. Santra, A. Michaelides, M. Scheffler, A. Tkatchenko, Phys. Rev. B 86 (2012) 245405-1-245405-6.
42 M. Luo, Q. Wang, G. Li, X. Zhang, L. Wang, Catal. Lett. 143 (2013) 454-462.
43 Y. Yu, B. Fonfé, A. Jentys, G. L. Haller, J. A. R van Veen, O. Y. Gutiérrez, J. A. Lercher, *J. Catal.*, 2012, **292**, 1-12.
44 H. Shi, O. Y. Gutiérrez, H. Yang, N. D. Browning, G. L. Haller, J. A. Lercher *ACS Catal.*, 2013, **3**, 328-338.
45 K. Ebitani, T. Tanaka, H. Hattori, Appl. Catal. A 102 (1993) 79-92.
46 T. Shishido, T. Tanaka, H. Hattori, J. Catal. 172 (1997) 24-33.
47 Y. Yu, O. Y. Gutiérrez, G. L. Haller, R. Colby, B. Kabius, A. Jentys, J. A. Lercher, *J. Catal.*, 2013, accepted.
48 Z. Paal, M. Muhler, R. Schogl, J. Catal. 143 (1993) 318-321
49 E. Iglesia, S.L. Soled, G.M. Kramer, J. Catal. 144 (1993) 238-253.
50 A. Dicko, X. Song, A. Adnot, A. Sayari, J. Catal. 150 (1994) 254-261.